Electromagnetic energy transport below the diffraction limit in periodic metal nanostructures

Stefan A. Maier, Pieter G. Kik, Mark L. Brongersma, Harry A. Atwater

Stefan A. Maier, Pieter G. Kik, Mark L. Brongersma, Harry A. Atwater, "Electromagnetic energy transport below the diffraction limit in periodic metal nanostructures," Proc. SPIE 4456, Controlling and Using Light in Nanometric Domains, (5 December 2001); doi: 10.1117/12.449534

SPIE.

Event: International Symposium on Optical Science and Technology, 2001, San Diego, CA, United States

Electromagnetic energy transport below the diffraction limit in periodic metal nanostructures

Stefan A. Maier, Pieter G. Kik, Mark L. Brongersma, and Harry A. Atwater
Thomas J. Watson Laboratory of Applied Physics, California Institute of Technology, Pasadena, CA

ABSTRACT

We investigate the possibility of using arrays of closely spaced metal nanoparticles as waveguides for electromagnetic energy below the diffraction limit of visible light. Coupling between adjacent particles sets up coupled plasmon modes that give rise to coherent propagation of energy along the array. A point dipole analysis predicts group velocities of energy transport that exceed 0.1c along straight arrays and shows that energy transmission through chain networks such as corners and tee structures is possible at high efficiencies. Although radiation losses into the far field are negligible due to the near-field nature of the coupling, resistive heating leads to transmission losses of about 3dB/500 nm for gold and silver particles. We confirmed the predictions of this analytical model using numeric finite difference time domain (FDTD) simulations. Also, we have fabricated gold nanoparticle arrays using electron beam lithography to study this type of electromagnetic energy transport. A modified illumination near field scanning optical microscope (NSOM) was used as a local excitation source of a nanoparticle in these arrays. Transport is studied by imaging the fluorescence of dye-filled latex beads positioned next to the nanoparticle arrays. We report on initial experiments of this kind.

Keywords: NSOM, near-field optics, metal nanoparticle, surface plasmon, plasmon waveguide

1. Introduction

In recent years, tremendous progress has been made in the miniaturization of optical devices due to advancements in key technologies such as planar waveguides and photonic crystals.[1,2] The size and density of optical devices employing these technologies is nonetheless limited by the diffraction limit $\lambda/2n$, which imposes a lower size limit of a few hundred nanometers on the optical mode size in integrated optical components.[1] Another limitation for further integration is the guiding geometry. Whereas photonic crystals allow for guiding of visible light around sharp corners[2], this is not possible in planar waveguides for which radiation leakage occurs at bends.[1]

A new method for guiding of electromagnetic energy that allows for device sizes below the diffraction limit has recently been proposed, relying on near-field interactions between closely spaced noble metal nanoparticles that can be efficiently excited at their surface plasmon frequency.[3] Using an analytical dipole model we showed that guiding of electromagnetic energy in arrays of closely spaced metal nanoparticles is due to near-field interactions between adjacent particles that sets up coupled plasmon modes leading to coherent propagation of energy along these arrays.[4,5] These plasmon waveguides allow for a variety of different subwavelength guiding geometries such as corners and tee-structures, and an all-optical switch can be designed employing interference effects.[4] We confirmed the guiding principle in a large scale analogue to plasmon waveguides in different geometries operating in the microwave regime and found close confinement of the electromagnetic energy to the guiding structures which in this case were composed of closely spaced metal rods.[6,7]

In this article, we report on our recent efforts to fabricate and characterize plasmon waveguides consisting of arrays of closely spaced gold nanoparticles. In section 2, we describe theoretical modeling of plasmon waveguides using both an analytical dipole model and numeric finite difference time domain (FDTD) methods. Section 3 describes the fabrication of plasmon waveguides using electron beam lithography and the optical characterization of the structures using a near field optical microscope (NSOM). Section 4 presents initial experimental results of these characterizations and discusses important issues for future work. We end by summarizing the present status of our work on plasmon waveguides.

Controlling and Using Light in Nanometric Domains, Aaron Lewis, H. Kumar Wickramasinghe, Katharina H. Al-Shamery, Editors, Proceedings of SPIE Vol. 4456 (2001)

2. Theoretical modeling of plasmon waveguides

2.1. The surface plasmon resonance of metal nanoparticles

Single noble metal nanoparticles interact strongly with visible light when excited at their dipole surface plasmon frequency.[8] he surface of the nanoparticle confines the conduction electrons inside the particle and sets up an effective restoring force leading to resonant behavior. Quasistatic Mie theory allows for an analytical description of this resonance for gold particles with diameters between 10-80 nm.[9]

The dipole surface plasmon resonance of small metal nanoparticles can be observed both in the far and in the near-field. Figure 1 shows calculated absorption, scattering and extinction efficiencies Q which are defined as the respective cross sections normalized by the geometrical cross section of a 30 nm Au particle in a medium with refractive index n=1.33 with the dipole surface plasmon peak occurring at 2.4 eV (~520 nm). This peak in the cross sections is due to a resonance in the polarizability α of the particle, which can be expressed for small spherical particles with radius R and dielectric function ε surrounded by a host with dielectric constant ε_m in the quasistatic limit as

$$\alpha = 4\pi\varepsilon_0 R^3 \frac{\varepsilon - \varepsilon_m}{\varepsilon + 2\varepsilon_m}. \tag{1}$$

The resonance occurs when the Fröhlich condition

$$\varepsilon(\omega) = -2\varepsilon_m. \tag{2}$$

is met and is thus influenced by the surrounding host. Particle shapes different from spheres can also be used to tune the resonance throughout the range of visible light.[8]

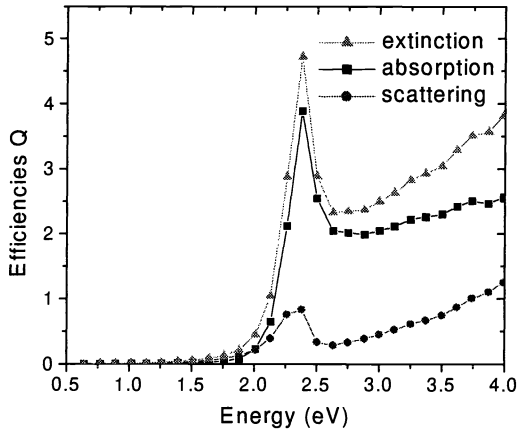

Figure 1. Optical extinction, absorption and scattering efficiencies for 30 nm Au spheres in a medium with refractive index n=1.33 calculated using quasistatic Mie theory. The efficiencies are defined as the respective cross sections divided by the geometrical cross section of the spheres.

The plasmon resonance can also be observed in the near-field in close vicinity of the particle using a photon scanning near field optical microscope. Noble metal particles illuminated by evanescent waves in total internal reflection geometry show an enhanced near field when excited at resonance.[10] This enhanced field can be probed with an NSOM tip brought in close proximity to the particle but can not be detected in the far field due to its evanescent character.

2.2. Dipole model of the energy transfer in plasmon waveguides

The resonance in the polarizability of a single noble metal nanoparticle at the surface plasmon resonance can be employed to guide electromagnetic energy along an array of such particles. The resonance increases the interaction strength between

adjacent particles. Indeed, it has been observed that a chain of closely spaced Au nanoparticles shows a collective behavior when excited in total internal reflection geometry.[11] We have modeled the near-field coupling between closely spaced particles that sets up coupled plasmon modes.[4,5] In the following, we will briefly discuss the nature of these modes.

When metal nanoparticles are spaced close together (separation a few tens of nanometers), as depicted in the inset of figure 2, the strongly distance dependent near-field term in the expansion of the electric dipole interaction dominates. The interaction strength and the relative phase of the electric field in neighboring particles are both polarization and frequency dependent. This interaction leads to coherent modes with a wavevector **k** along the nanoparticle array. One can calculate a dispersion relation for energy propagation along the array by taking into account nth nearest neighbor interactions via a polarization dependent interaction frequency ω_1 derived from the electromagnetic interaction term and the plasmon dipole resonance at ω_0 of a single nanoparticle. Figure 2 shows the results of such a calculation for modes with the dipole oscillation along the chain (longitudinal modes L) and for modes polarized perpendicular to the chain (transverse modes T). Calculations were done including nearest-neighbor coupling only (solid lines) and including up to five nearest neighbors in the coupling term (dashed lines) for an infinite linear array of metal nanoparticles. The inclusion of up to five nearest neighbors has little effect on the dispersion curves, confirming that the interaction is dominated by nearest neighbor coupling. For both polarizations, the propagation velocity of the guided energy given by the slope $d\omega/d\mathbf{k}$ of the dispersion relation is highest at the resonance frequency ω_0. At this frequency, the wavelength of the guided mode is four particle spacings. Calculations for 50 nm silver and gold spheres with a center-to-center distance of 75 nm show energy propagation velocities of about 10% of the speed of light. This is ten times faster than the saturation velocities of electrons in typical semiconductor devices.

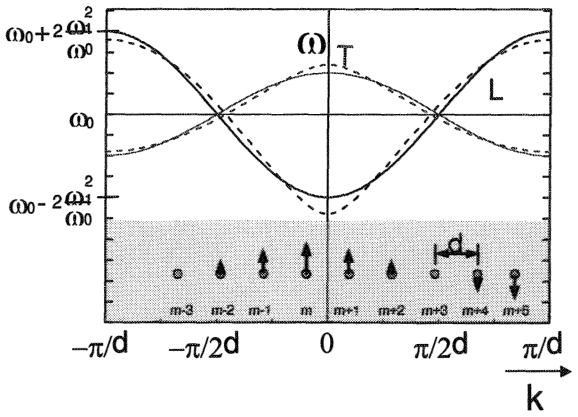

Figure 2. Dispersion relation for plasmon modes in a linear chain (see inset) of metal nanoparticles, showing the twofold degenerate branch corresponding to transverse modes (T) and the branch corresponding to longitudinal modes (L). Results are shown for calculations incorporating nearest-neighbor interactions only (solid curve), and including up to fifth-nearest neighbor interactions (dotted curve). The small difference in the dispersion curves illustrates that mode propagation in plasmon waveguides is dominated by near-field interactions.

Another important parameter in waveguide design aside from the dispersion relation is loss. Internal and radiation damping are also accounted for in the model.[4,5] In plasmon waveguides, the loss is due to internal damping of the plasmon oscillation in each nanoparticle. This damping due to resistive heating was shown to induce transmission losses of about 3dB/500 nm.[4,5] Losses due to radiation can be neglected in these waveguides due to the near-field nature of the coupling.

Using this analytical dipole model, we analyzed the transmission characteristics of several circuit elements such as 90 degree corners and tee structures for signal splitting.[4,5] We found that signals can be guided through such structures with negligible radiation losses due to the fact that the coupling is dominated by near-field terms. Power transmission coefficients for the guiding of energy around sharp bends are highly polarization dependent and are typically >50%. Due to the coherent nature of the propagation, it is also possible to design all-optical switches that rely on interference effects, such as Mach-Zehnder interferometers.[4]

2.3. FDTD simulations of plasmon waveguides

To test the validity of our analytical dipole approximation model, we conduct FDTD simulations of plasmon waveguides in a variety of geometries. Figure 3 shows results of our simulations for a chain of seven 50 nm Au particles in air with a center-to-center distance of 75 nm along the x-direction. A transverse plasmon mode is locally excited via a dipole pointing in the z-direction on the left side of the particle chain at the surface plasmon frequency of a single particle located at 481 nm. The plots show the z component of the electric field in the x-y plane at z=0 at different time points t_x after the dipole field is turned on at time t_1. The interval between time points is 1.9×10^{-16}s which is a tenth of the dipole oscillation period.

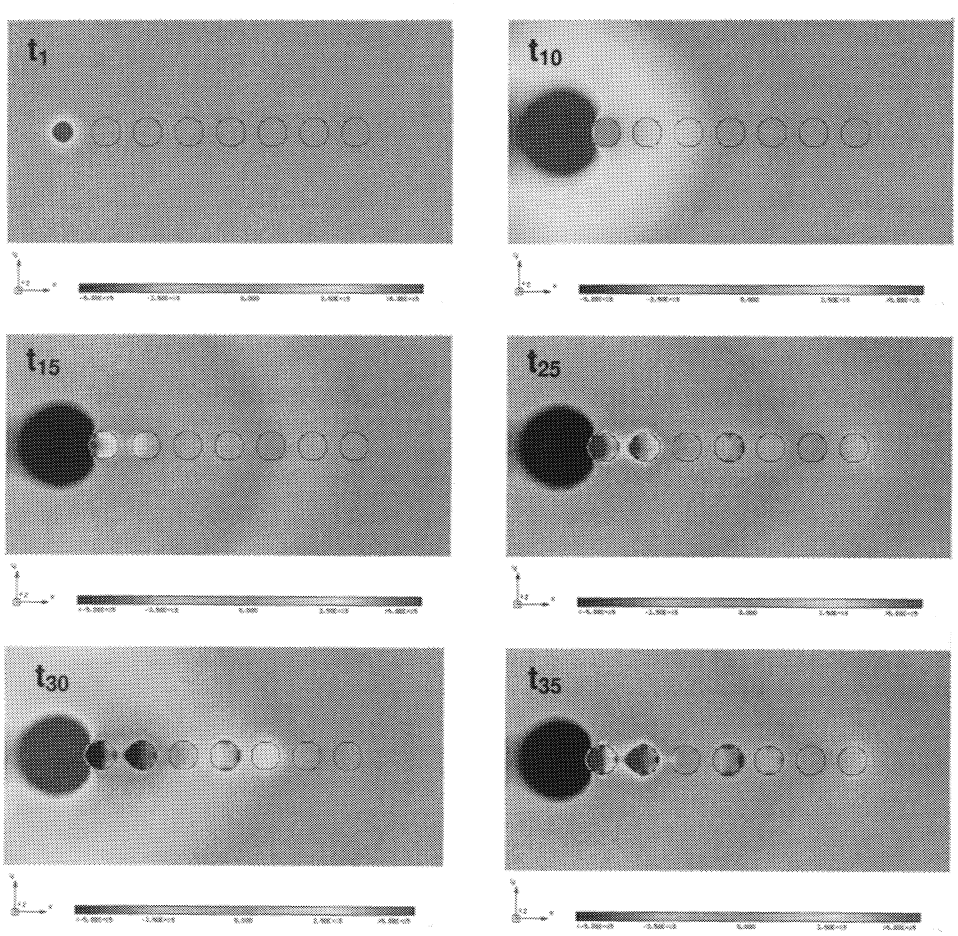

Figure 3. FDTD simulations of a chain of seven 50 nm Au particles with a center-to-center distance of 75 nm in air. The plots show the z-component of the evolving electric field on a linear scale after the structure is locally excited via a dipole source at 481 nm placed on the left side of the chain

The electric field is clearly confined to the guiding nanoparticle array. Careful examinations of our initial calculations confirm a power loss along the arrays on the order of 3dB/500 nm as predicted by our analytical dipole model. The simulations also suggest a wavelength of the guided wave of about 6 particle spacings, whereas the dispersion relation in figure 2 suggests a wavelength of 4 particle spacings for resonant excitations. The structure is possibly excited above its resonance frequency, which means that the surface plasmon frequency of a chain of Au particles is lower than the resonance frequency of a single particle which in air is located at 481 nm. This shift of the plasmon frequency is due to dipole-dipole interactions between closely spaced nanoparticles and has been previously observed in the far field.[12]

We intent to extend our initial FDTD simulations to plasmon waveguides composed out of longer chains of metal particles imbedded in various dielectric hosts and to study their transmission characteristics for different particle shapes and spacings.

3. Fabrication of plasmon waveguides and experimental setup

3.1. Fabrication of plasmon waveguides

Since the position and width of the surface plasmon resonance of metal nanoparticles depend on their shape and size, the applied fabrication methods should produce a narrow size distribution of the individual particles. Furthermore, a regular particle spacing is crucial for the transport properties due to the strong distance dependence of the electromagnetic near field. A distribution in interparticle distances and sizes will lead to wave reflections in the array.

We have fabricated gold nanoparticles with diameters of 50 nm. The gold plasmon resonance is conveniently located around the 514 nm line of an Argon laser for excitation if the structure is deposited on a glass substrate. The center-to-center distance between adjacent particles was chosen to be 3R, where R is the particle radius, to optimize the guiding properties of the structures.[3] We fabricated nanoparticle structures in several geometries using electron beam lithography and liftoff on ITO doped glass. Figure 4a and b show straight nanoparticle arrays each consisting of 80 nanoparticles. The individual arrays are spaced one micron apart to eliminate cross talk. Figure 4c shows a 90 degree corner consisting of 20 nanoparticles in each arm. The SEM pictures confirm a narrow size distribution and a regular spacing of the individual particles which have an almost circular cross section. Figure 4d shows solid Au nanowires which were also fabricated to compare their optical properties to nanoparticle plasmon waveguides.

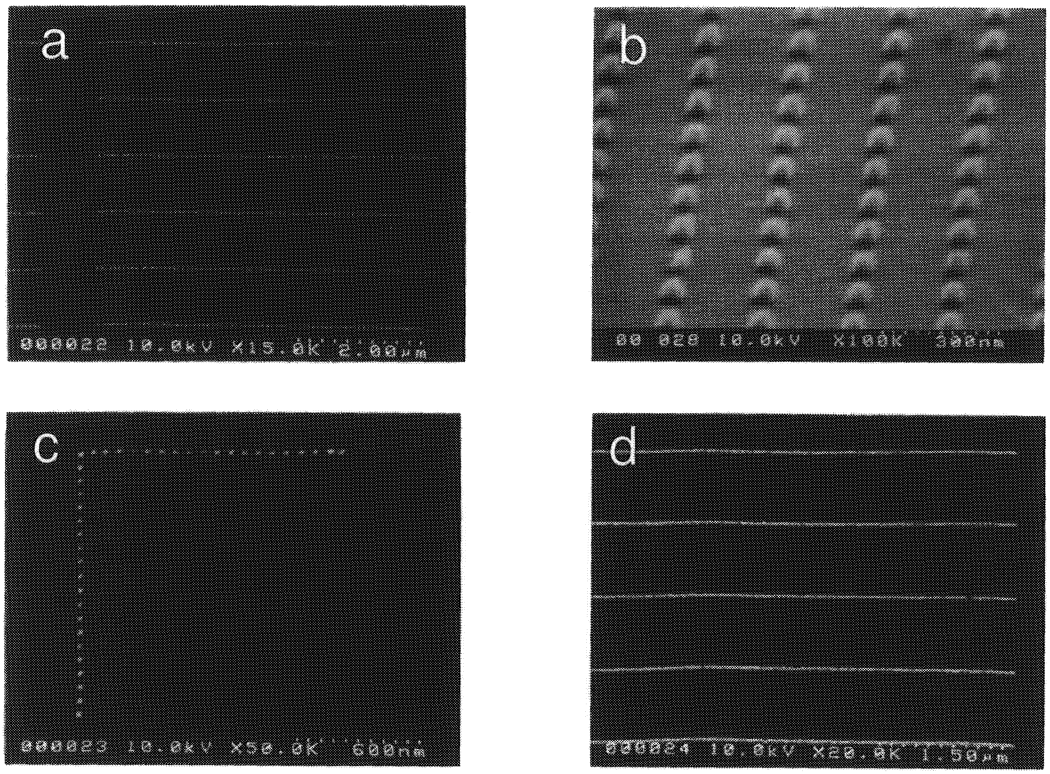

Figure 4. SEM pictures of nanoscale structures fabricated using electron beam lithography. **a)** plasmon waveguides consisting of 80 Au nanoparticles. **b)** 70° tilted view of the same structures, showing that the individual particles are about 50 nm in diameter and have almost circular cross sections. **c)** 90 degree corner plasmon waveguide. **d)** solid Au nanowires for comparison with nanoparticle waveguides

3.2. An illumination mode NSOM for excitation and characterization of plasmon waveguides

In order to examine the transport properties of plasmon waveguides for electromagnetic energy, a local excitation of a single nanoparticle in the array is necessary as opposed to the excitation of the array as a whole using broad beam illumination. To accomplish this we want to locally excite the dipole resonance of a single Au particle in our fabricated structures using the tip of an illumination mode NSOM. Figure 5a depicts the basic idea of our experiment. Power transport away from the excited Au nanoparticle is probed via the careful placement of 60 nm latex beads filled with fluorescent dyes

in close proximity to the guiding Au structures. The dyes absorb at 520 nm near the plasmon resonance of Au particles and emit radiation at 580 nm, which is detected in the far field. This scheme allows the observation of energy transport properties of the plasmon waveguides since energy gets transferred from the illuminating tip to the plasmon waveguide, gets transferred along the nanoparticle structure and finally excites a fluorescent bead placed at a sufficient distance from the excitation source.

We modified a commercially available illumination mode NSOM for fluorescence detection, as depicted in figure 5b. The sample is locally illuminated at 514 nm using an Argon ion laser through a metallized cantilevered NSOM tip with a 50 nm aperture. The transmitted light is collected via a high numerical aperture objective and analyzed via a CCD camera, an avelanche photo diode (APD) or a spectrometer. The whole system is built into an inverted optical microscope. Different filter setups allow for detection of either the scattered laser light or the fluorescence. A beam bounce detection systems and atomic force microscope feedback electronics allow for the simultaneous generation of a topographical image when the tip scans the surface.

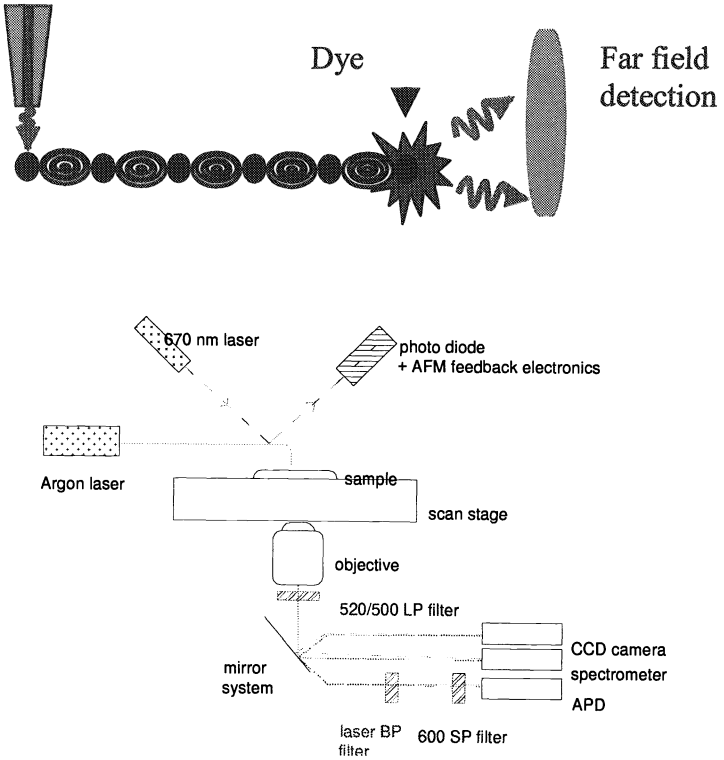

Figure 5. a) Schematic of the setup for the characterization of the transport properties of plasmon waveguides. **b)** Illumination mode NSOM setup

4. Initial results of the optical characterization of plasmon waveguides

Figure 6 shows the topography and transmitted laser light NSOM signal obtained by scanning our fabricated nanoscale structures with the NSOM system described in section 3.2. Figure 6a shows the topography of solid 50 nm Au nanowires as the height and the transmitted laser light as the grayscale colors in a combined topography/NSOM 3D plot. The solid nanowires lead to a decrease in the transmitted laser light which is shifted spatially in respect to the height signal but shows the same periodicity. We attribute this shift to illumination under an angle to the direction of normal incidence which is due to the specific tip geometry employed in our setup. Figure 6b shows both the topography and the transmitted laser light NSOM signal of plasmon waveguides consisting of 50 nm Au particles with a center-to-center distance of 75 nm. Individual particles can be resolved in the topographic image even though the tip radius of 50 nm is rather large compared to

conventional silicon AFM cantilevered tips. The topographic image also shows randomly deposited 60 nm latex beads in the proximity of the structure. The NSOM signals shows decreased transmission of illuminating laser light when the tip is above the particle structures, even though the signal-to-noise ratio is not as good as with scans over solid Au nanowires.

A first demonstration of the capabilities of our NSOM system in detecting fluorescent radiation is given in figure 7. Shown is a 3D plot of a scan of plasmon waveguides composed of 50 nm Au particles with a center-to-center distance of 75 nm as discussed above. The scan area includes 10 waveguides separated by 1 micron. The topography of the 3D plot shows the height signal with an imaging artifact in the center of the plot. The grayscale shows the intensity of the fluorescence signal detected using an avalanche photo diode when the area is illuminated at 514 nm using a 50 nm NSOM tip. The fluorescence of randomly deposited dye particles in the rear of the picture next to a waveguide can be clearly discerned. Yet no fluorescent signal is detected when the NSOM tip is located on top of the nanoparticle array. This could be attributed to the fact that the dye particles are not close enough to the waveguide in order to allow for energy transfer. Nonetheless this experiment shows that our envisioned experiment discussed above should be possible with our system.

We are currently working on an improved deposition method for the fluorescent latex beads which will place them closer to the plasmon waveguides to allow for energy transfer between the Au nanoparticles and the dyes. In particular, we are investigating the possibility to manipulate the latex beads with the tip of an atomic force microscope in order to push them in close proximity to the waveguides. Our combined AFM/NSOM system has proven to be capable of resolving plasmon waveguides and detecting dye fluorescence, so future experiments should provide considerable insight into the transport properties of plasmon waveguides.

4. Conclusion

Plasmon waveguides built up out of arrays of closely spaced noble metal nanoparticles can be used to fabricate nanoscale optical devices with a lateral mode size well below the diffraction limit of visible light. Analytical models in the dipole limit show that the transport of electromagnetic energy takes place at group velocities as high as 10% of the velocity of light for gold or silver nanoparticles. Basic circuits elements such as corners, highly efficient splitters and switches can be realized. FDTD simulations of plasmon waveguides confirm their guiding properties and show transmission losses of about 3 dB/500 nm. Fabrication of plasmon waveguides is possible using electron beam lithography, and their transport properties can be characterized with an illumination mode NSOM. Their subwavelength size and variable geometry make plasmon waveguides promising candidates for future highly integrated optical devices.

Acknowledgements

This work was sponsored by the National Science Foundation.

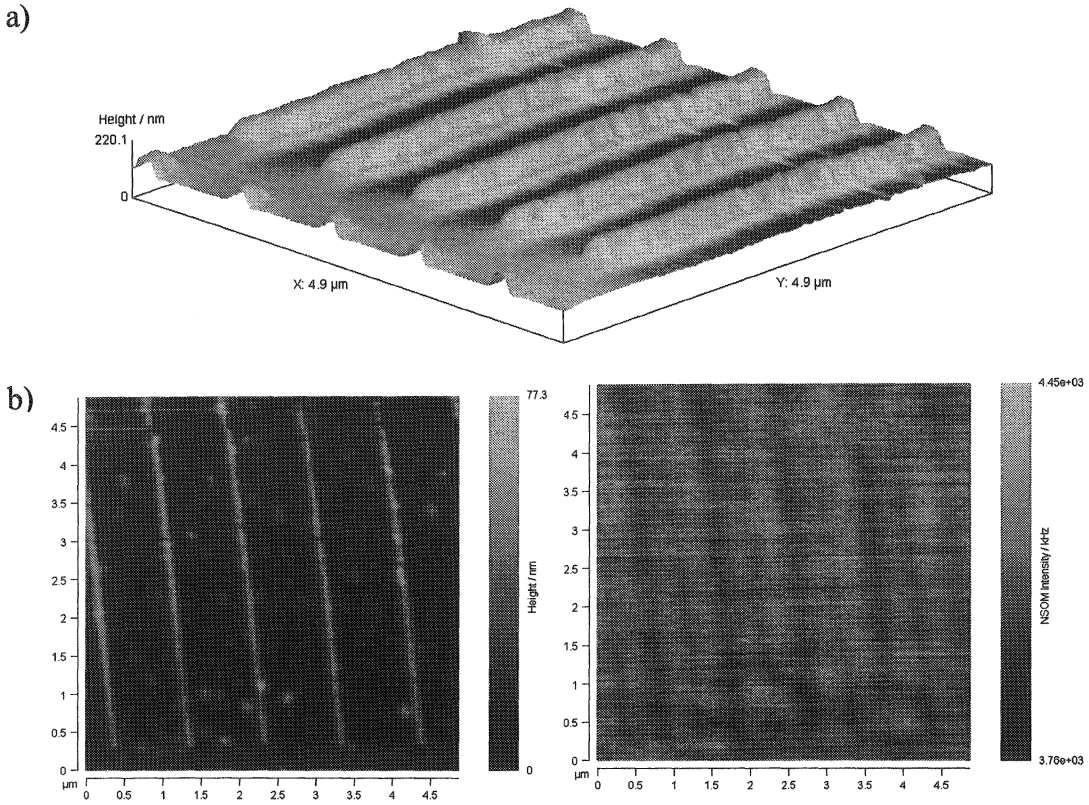

Figure 6. a) Topography and transmitted laser light NSOM signal for 50 nm solid Au nanowires. The grayscale shows the intensity of the transmitted laser light, with reduced transmission at the left side of each wire **b)** Topography and transmitted laser light NSOM signal for straight plasmon waveguides with individual particles spaced 75 nm apart. Individual Au particles can be resolved in the topography image which also shows randomly deposited latex beads in proximity of the nanoparticle structures. The NSOM signal shows reduced transmission of the illuminating laser light at the plasmon waveguide position.

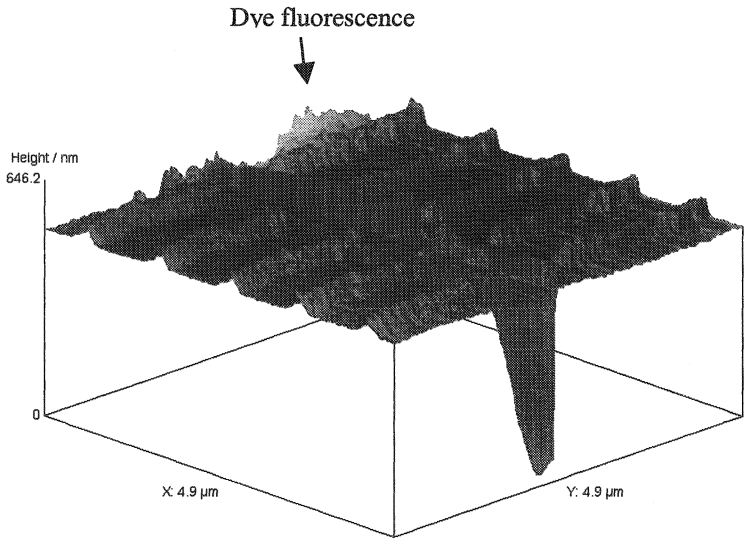

Figure 7. Topography and fluorescent NSOM signal of plasmon waveguides consisting of 50 nm Au particles with fluorescent latex beads in proximity to the structures. A fluorescent signal is detected when the tips scans over the dyes at the rear of the picture.

References

1. B.E.A. Saleh and M.C. Teich, *The Fundamentals of Photonics*, Wiley, New York, 1991
2. A. Mekis, J.C. Chen, I. Kurland, S. Fan, P.R. Villeneuve, and J.D. Joannopoulos, "High transmission through sharp bends in photonic crystal waveguides", *Physical Review Letters* **77**, pp 3787-3790, 1996
3. M. Quinten, A. Leitner, J.R. Krenn, and F.R. Aussenegg, "Electromagnetic energy transport via linear chains of silver nanoparticles", *Optics Letters* **23**, pp. 1331-1333, 1998
4. M.L. Brongersma, J.W. Hartman, and H.A. Atwater, "Electromagnetic energy transfer and switching in nanoparticle chain arrays below the diffraction limit", *Physical Review B* **62**, pp. R16356-R16359, 2000
5. S.A. Maier, M.L. Brongersma, P.G. Kik, and H.A. Atwater, "Plasmonics – a route to nanoscale optical devices", *Advanced Materials*, to be published 2001
6. S.A. Maier, M.L. Brongersma, and H.A. Atwater, "Electromagnetic energy transport along arrays of closely spaced metal rods as an analogue to plasmonic devices", *Applied Physics Letters* **78**, pp. 16-18, 2001
7. S.A. Maier, M.L. Brongersma, and H.A. Atwater, "Electromagnetic energy transport along Yagi arrays", *Mat. Res. Soc. Symp. Proc.* **637**, E2.9.1, 2001
8. U. Kreibig and M. Vollmer, *Optical Properties of Metal Clusters*, Springer, New York, 1994
9. G. Mie, "Beiträge zur Optik trüber Medien speziell kolloidaler Metallösungen", *Annalen der Physik* **25**, pp. 377-445, 1908
10. J.R. Krenn, J.C. Weeber, A. Dereux, E. Bourillot, J.P. Goudonnet, B. Schider, A. Leitner, F.R. Aussenegg, C. Girard, "Direct observation of localized surface plasmon coupling", *Physical Review B* **60**, pp. 5029-5033, 1999
11. J.R. Krenn, A. Dereux, J.C. Weeber, E. Bourillot, Y. Lacroute, J.P. Goudonnet, G. Schider, W. Gotschy, A. Leitner, F.R. Aussenegg, C. Girard, "Squeezing the optical near-field zone by plasmon coupling of metallic nanoparticles", *Physical Review Letters* **82**, pp. 2590-2593, 1999
12. B. Lamprecht, G. Schider, R.T. Lechner, H. Ditlbacher, J.R. Krenn, A. Leitner, and F.R. Aussenegg, "Metal nanoparticle gratings: Influence of dipolar particle interaction on the plasmon resonance", *Physical Review Letters* **84**, pp. 4721-4724, 2000